Automatica 130 (2021) 109662

Contents lists available at ScienceDirect

Automatica

journal homepage: www.elsevier.com/locate/automatica

Comparison of guaranteed state estimators for linear time-invariant systems☆

Matthias Althoff [a], Jagat Jyoti Rath [b,*]

[a] Department of Informatics, Technische Universität München, 80333 München, Germany
[b] Department of Mechanical and Aero-Space Engineering, Institute of Infrastructure Technology Research and Management, Ahmedabad 380026, India

ARTICLE INFO

Article history:
Received 5 December 2019
Received in revised form 3 November 2020
Accepted 21 March 2021
Available online 14 May 2021

Keywords:
Guaranteed state estimation
Set-based observers
Strip-based observers
Set-propagation observers
Interval observers
Zonotopes
Ellipsoids
Constrained zonotopes
Comparison
Linear time-invariant systems

ABSTRACT

Guaranteed state estimation computes the set of possible states of dynamical systems given the bounds of model uncertainties, disturbances, and noises. For the first time, we evaluate and compare a broad class of guaranteed state estimators for linear time-invariant systems regarding scalability, accuracy, and real-time applicability. In particular, we consider strip-based observers, set-propagation observers, and interval observers. The performance of most guaranteed state estimators is significantly affected by the chosen set representation. Zonotopes have emerged as a popular set representation since important operations such as linear maps and Minkowski sum can be computed exactly and efficiently. Furthermore, we provide comparisons with ellipsoids and constrained zonotopes as set representations. The comparison is conducted on various models for state estimation of autonomous vehicles.

© 2021 Elsevier Ltd. All rights reserved.

1. Introduction

Systems are becoming increasingly autonomous, such as automated road vehicles, surgical robots, automatic operation of smart grids, and collaborative human–robot manufacturing. Hence, they are increasingly safety-critical and/or operation-critical (Mitra, Wongpiromsarn, & Murray, 2013; Rajkumar, Lee, Sha, & Stankovic, 2010). Controlling these systems requires state observers, because the full system state is typically not measured due to, e.g., a lack of measuring devices, packaging problems, or just economic reasons. While estimating the most likely state is sufficient for non-critical applications, critical systems require the entire set of possible states from guaranteed state estimation (Alamo, Bravo, & Camacho, 2005; Bertsekas & Rhodes, 1971; Blanchini & Miani, 2008; Chisci, Garulli, & Zappa, 1996; Combastel, 2015b; Schweppe, 1968). The set of possible states can be used to rigorously predict future behaviors (Althoff & Dolan, 2014; Falcone, Ali, & Sjöberg, 2011), perform robust control (Limon, Alvarado, Alamo, & Camacho, 2010; Schürmann, Kochdumper, & Althoff, 2018), perform conformance checking (Roehm, Oehlerking, Woehrle, & Althoff, 2016), or apply robust fault detection (Xiong, 2013). We consider rigorous state estimation of linear time-invariant systems, which can also be used to observe nonlinear systems when using conservative linearization techniques, see, e.g., Althoff, Stursberg, and Buss (2008) and Combastel (2005).

Types of set-based observers: In essence, three types of set-based observers have been developed in the last decades: strip-based observers, set-propagation observers, and interval observers. Strip-based observers propagate the set of possible states forward using reachability analysis (Althoff, 2010), followed by intersecting it with strips of possible states from measurements; see, e.g., Alamo et al. (2005), Blanchini and Miani (2008), Chisci et al. (1996), Schweppe (1968). Set-propagation observers do not require intersecting sets and propagate sets based on the joint use of reachability analysis and the concept of a Luenberger observer (Combastel, 2015b; Pourasghar, Puig, & Ocampo-Martinez, 2019). Finally, interval observers consist of two separate observers that provide an upper and lower bound so that state variables are bounded within intervals (Efimov, Raïssi,

☆ The authors gratefully acknowledge the partial financial support of this work by the European Research Council (ERC) project justITSELF under grant agreement No 817629 and the Ford Motor Company, Germany. The material in this paper was not presented at any conference. This paper was recommended for publication in revised form by Associate Editor Andrea Garulli under the direction of Editors Sonia Martinez, Torsten Söderström.

* Corresponding author.
E-mail addresses: althoff@tum.de (M. Althoff), jagat.rath@iitram.ac.in (J.J. Rath).

https://doi.org/10.1016/j.automatica.2021.109662
0005-1098/© 2021 Elsevier Ltd. All rights reserved.

Chebotarev, & Zolghadri, 2013; Gouzé, Rapaport, & Hadj-Sadok, 2000; Mazenc & Bernard, 2011; Raïssi & Efimov, 2018; Zheng, Efimov, & Perruquetti, 2016). We would like to mention that historically, strip-based observers are often also referred to as set membership observers; however, in principle all guaranteed observers compute set memberships. Also, some papers bound their states by intervals and refer to them as interval observers; however, we prefer to categorize the observers algorithmically rather than based on the set representation.

Typical set representations: One of the barriers to wide-spread use of guaranteed state estimation is their higher computational cost compared to classical observers. Choosing an appropriate set representation is a key design choice. For instance, by modeling sets as the convex hull of vertices, an axis-aligned box in $\mathbb{R}^n$ would already have 2^n vertices so that just storing a single set is infeasible in high-dimensional spaces. Besides the representation size, it is important that relevant operations can be efficiently computed or over-approximated. Guaranteed state estimation requires linear maps and Minkowski sum. For strip-based approaches, one additionally requires intersection. The importance of set representations led to exploring ellipsoids (Bertsekas & Rhodes, 1971; Blanchini & Miani, 2008; Chabane, 2015; Schweppe, 1968), zonotopes (Alamo et al., 2005; Combastel, 2015b; Pourasghar et al., 2019; Puig, Cuguero, & Quevedo, 2001), constrained zonotopes (Rego, Raffo, Scott, & Raimondo, 2020; Rego, Raimondo, & Raffo, 2018; Scott, Raimondo, Marseglia, & Braatz, 2016), and polytopes (Kostousova, 1998). However, ellipsoids are not closed under Minkowski sum and intersection, requiring to compute overly large over-approximations (Durieu, Walter, & Polyak, 2001; Gollamudi, Nagaraj, Kapoor, & Huang, 1996; Polyak, Nazin, Durieu, & Walter, 2004). To obtain tighter sets, polytopes have been suggested at the expense of large computational costs, e.g., computing the Minkowski sum of two polytopes for $n = 20$ is computationally infeasible. To reduce computation time, parallelotopes as a special class of polytopes are discussed in Chisci et al. (1996) and Kostousova (1998). However, paralellotopes are also not closed under Minkowski sum, resulting in conservative results. While constrained zonotopes can represent any polytope and perform Minkowski sums more efficiently, it requires linear programming to compute the ranges of values in a given direction. To obtain a good balance of accuracy and computational costs, zonotopes (Althoff, 2010; Kühn, 1998) are widely used in recent works since they are closed under Minkowski sum and linear maps. Due to the recent popularity of zonotopic state observers, we focus on this set representation subsequently.

Zonotopic strip-based observers: Although zonotopes are not closed under intersection like ellipsoids, intersection of zonotopes can be efficiently over-approximated. Previous works mostly differ in how the intersection is over-approximated: (a) singular value decomposition is used in Combastel (2003), which is computationally efficient, but does not optimize a particular performance metric; (b) segment minimization and volume minimization (Alamo et al., 2005) overcome limitations of the singular-value-decomposition approach. However, segment minimization leads to conservative results when handling uncertainties across multiple dimensions (Le, Alamo, Camacho, Stoica and Dumur, 2011; Le, Stoica, Alamo, Camacho, & Dumur, 2013b), while volume minimization is computationally expensive (Le, Alamo et al., 2011). Combining the merits of both approaches, a novel P-radius minimization technique provides a good ratio of accuracy and computation costs (Le, Alamo et al., 2011; Le, Alamo, Camacho, Stoica, & Dumur, 2012; Le et al., 2013b; Le, Stoica, Dumur, Alamo and Camacho, 2011). Since the previously-mentioned designs lead to conservative results for high-dimensional systems, a novel P-radius-based estimation is proposed in Le, Stoica, Alamo, Camacho, and Dumur (2013a) for uncertain multi-output linear systems considering all measurements simultaneously. The continuous improvement of zonotopic strip-based observers led to several applications for parameter estimation and fault diagnosis, among others (Blesa, Puig, Romera, & Saludes, 2011; Puig, 2010).

Zonotopic set-propagation and interval observers: Let us subsequently survey zonotopic set-propagation observers. P-radius minimization has also been applied to set-propagation observers (Tang et al., 2018; Wang, Puig, & Cembrano, 2018b; Wang, Zhou, Puig, Cembrano, & Wang, 2017). Similarly, in Combastel (2015b), a special type of set-propagation observer is proposed to minimize the Frobenius norm of the estimation error while ensuring robustness and making explicit links with Kalman filters. Zonotopic set-propagation observers have also been applied to fault detection (Blesa, Rotondo, Puig, & Nejjari, 2014; Combastel, 2015a; Wang & Puig, 2016; Wang, Puig, & Cembrano, 2018a), parameter estimation (Wang, Kolmanovsky and Sun, 2018), and feedback control problems (Witheephanich, Orihuela, Garcia, & Escano, 2016). To avoid the wrapping effect of zonotopic observers, an H-infinity interval observers is presented in Tang, Wang, Wang, Raïssi, and Shen (2019).

Contributions: In summary, many aspects of zonotopic state observer design, such as accuracy, scalability, and computational costs are not yet compared in detail. A comparative analysis between zonotopic strip-based and set-propagation observers for a single-output system was presented in Pourasghar, Puig, and Ocampo-Martinez (2016).[1] Extending this work, a comparison analysis for fault detection using zonotopic strip-based and set-propagation observers is performed in Pourasghar et al. (2019).[1] For the first time, we present a comprehensive comparison of different zonotopic observers for linear time-invariant systems with the following features:

- Comparison between strip-based observers, set-propagation observers, and interval observers.
- Comparison between observers using different minimization techniques, such as volume minimization, F-radius minimization, P-radius minimization, and H-infinity minimization.
- Comparison between zonotopes, constrained zonotopes, and ellipsoids as set representations.
- Consideration of single-output and multi-output estimation.
- Scalability analysis and assessment of real-time capabilities.
- Performance analysis with respect to different parameter settings, such as the used zonotope order.

For performing the comparison, we consider vehicle-side-slip estimation for road vehicles (Wang, Bevly, & Rajamani, 2015).

2. Preliminaries

Let us first give a brief introduction to strip-based observers, set-propagation observers, and interval observers for linear time-invariant systems.

2.1. Set representations

Before we introduce specific sets, let us first introduce the following set operations for $\mathcal{S}_1, \mathcal{S}_2 \subset \mathbb{R}^n$:

- *Linear map*: $M\mathcal{S}_1 = \{Ms_1 \mid s_1 \in \mathcal{S}_1\}, M \in \mathbb{R}^{n\times n}$.
- *Minkowski sum*: $\mathcal{S}_1 \oplus \mathcal{S}_2 = \{s_1 + s_2 \mid s_1 \in \mathcal{S}_1, s_2 \in \mathcal{S}_2\}$.

[1] That work refers to strip-based observers as set membership observers and to set-propagation observers as interval observers.

One of the simplest set representations are intervals: $[\underline{x}, \overline{x}] = \{x \in \mathbb{R} \mid \underline{x} \leq x \leq \overline{x}\}$. An axis-aligned box is an interval vector $\left[\ [\underline{x}_1, \overline{x}_1], [\underline{x}_2, \overline{x}_2], \ldots [\underline{x}_n, \overline{x}_n]\ \right]^T$. We define the unit interval as $\mathcal{B} = [-1, 1]$ and the unit box in $\mathbb{R}^n$ as $\mathcal{B}^n$. A more general set representation than intervals are polyhedra, which can be defined as the intersection of m half-spaces (H-representation) (Chabane, 2015, eq. 3.20):

$$\mathcal{P} = \left\{ x \in \mathbb{R}^n \middle| Dx \leq d \right\}, \tag{1}$$

where $D \in \mathbb{R}^{m \times n}$ and $d \in \mathbb{R}^m$. A bounded polyhedral set is called a polytope. A class of centrally-symmetric polytopes are called zonotopes and are represented as

$$\mathcal{Z} = c \oplus G\mathcal{B}^r,$$

where $c \in \mathbb{R}^n$ is the center, $G \in \mathbb{R}^{n \times r}$ is a matrix representing the generators, and r/n is the order of the zonotope (Althoff, 2010, Sec. 2.1).[2] When adding a linear constraint $A\xi = b$ to zonotopes, where $A \in \mathbb{R}^{n_c \times r}$, $b \in \mathbb{R}^{n_c}$, and ξ is the vector that is mapped by the generator matrix, one obtains a constrained zonotope (Scott et al., 2016, Def. 3):

$$\mathcal{CZ} = \{c + G\xi \,|\, \xi \in \mathcal{B}^r, A\xi = b\}.$$

Finally, we present ellipsoids, which are defined by a symmetric positive definite matrix $H = H^T \succ 0$, and the center $c \in \mathbb{R}^n$ as (Chabane, 2015, eq. 3.33)

$$\mathcal{E}(H, c) = \left\{ x \in \mathbb{R}^n \;\middle|\; (x - c)^T H (x - c) \leq 1 \right\}.$$

2.2. Cost functions

To minimize the size of the estimated sets, we define the following costs of a zonotope $\mathcal{Z} = c \oplus G\mathcal{B}^r$:

- **Volume:** The volume of a zonotope (see Alamo et al. (2005, Sec. 6.2)).
- **F_P-radius:** Given a symmetric weighting matrix $P \in \mathbb{R}^{n \times n}$, $P = P^T \succ 0$, the F_P-radius is the weighted Frobenius norm of G (Combastel, 2015b, Def. 2):

  $$F_P = \|G\|_{F,P} = \sqrt{\text{trace}(G^T P G)}.$$

  When the weighting matrix is the identity, i.e., $P = I \in \mathbb{R}^{n \times n}$, we say that the F-radius instead of the F_P radius is obtained.
- **P-radius:** For a positive definite symmetric matrix $P = P^T \succ 0$, the P-radius (Le et al., 2013b, Sec. 2) is

  $$\Theta = \max_{z \in \mathcal{Z}}(\|z - c\|_P^2) = \max_{z \in \mathcal{Z}}((z - c)^T P (z - c)).$$

2.3. Problem statement

We consider discrete-time, linear, time-invariant disturbed systems, with state $x_k \in \mathbb{R}^n$, input $u_k \in \mathbb{R}^{n_u}$, output $y_k \in \mathbb{R}^{n_y}$, disturbance $w_k \in \mathbb{R}^{n_w}$, and sensor noise $v_k \in \mathbb{R}^{n_v}$ at step k:

$$\begin{aligned} x_{k+1} &= Ax_k + Bu_k + w_k, \\ y_k &= Cx_k + v_k, \end{aligned} \tag{2}$$

where A, B, and C are matrices of proper dimensions. It is assumed that the system is observable and that the disturbance is bounded by the zonotopes $\mathcal{W} = E\mathcal{B}^{n_w}$ and the noise is bounded by the set $\mathcal{V} = F\mathcal{B}^{n_v}$. Please note that other works use $\tilde{E}\tilde{w}_k$ and $\tilde{F}\tilde{v}_k$ instead of w_k and v_k in (2), however, this is not a more general case since one can simply choose $\mathcal{W} = \tilde{E}\tilde{\mathcal{W}}$ and $\mathcal{V} = \tilde{F}\tilde{\mathcal{V}}$. A possible way to automatically find proper sets $\mathcal{W}$ and $\mathcal{V}$ is through conformance checking, see, e.g., Kochdumper et al. (2020), Liu and Althoff (2018) and Roehm, Oehlerking, Woehrle, and Althoff (2019). For a given state x_k, input u_k, and disturbance w_k, let us denote the next state of (2) by $\chi(x_k, u_k, w_k)$.

Our objective is to find the sets of possible states at time step k, which we define inductively starting with the initial set $\mathcal{S}_0 \subset \mathbb{R}^n$:

$$\begin{aligned} \mathcal{S}_k = \Big\{ x_k = \chi\left(x_{k-1}, u_{k-1}, w_{k-1}\right) \Big| x_{k-1} \in \mathcal{S}_{k-1}, w_{k-1} \in \mathcal{W}, \\ v_k \in \mathcal{V}, y_k = Cx_k + v_k \Big\}. \end{aligned} \tag{3}$$

We aim at computing an over-approximation of $\mathcal{S}_k$ that minimizes the previously-presented cost functions. This goal is pursued differently for the strip-based, set-propagation, and interval observers presented subsequently.

2.4. Strip-based observers

Strip-based observers first propagate the possible set of states according to the system dynamics, which is intersected by the set of possible states due to the current measurement:

(1) *Prediction*: By evaluating (2) in a set-based fashion, one obtains the next set of possible states (Le et al., 2013b, Def. 2):

$$\mathcal{S}^p = A\mathcal{S}_{k-1} \oplus Bu_{k-1} \oplus \mathcal{W}.$$

(2) *Measurement update*: Due to the linear measurement function in (2), the possible states from the measurement of the jth output signal $y_{k,j}$ at time step k are bounded by a strip of width σ_j (Alamo et al., 2005, Property 2):

$$\hat{\mathcal{S}}_j = \left\{ x \in \mathbb{R}^n \middle| |C_j x - y_{k,j}| \leq \sigma_j \right\}, \tag{4}$$

where C_j is the jth row of the measurement matrix C in (2) and σ is the symmetric bound of the box enclosing the sensor noise: $[-\sigma, \sigma] = \text{BOX}(\mathcal{V})$. The entire measurement set $\mathcal{S}_y$ is computed by over-approximating the intersection of all strips:

$$\hat{\mathcal{S}} \subseteq \hat{\mathcal{S}}_1 \cap \hat{\mathcal{S}}_2 \ldots \cap \hat{\mathcal{S}}_{n_y}. \tag{5}$$

(3) *Correction*: The set consistent with the propagated set $\mathcal{S}^p$ and the measurement set $\hat{\mathcal{S}}$ is simply obtained by intersection, which is often over-approximated for computational efficiency (Alamo et al., 2005, Sec.3):

$$\mathcal{S}_k \supseteq \mathcal{S}^p \cap \hat{\mathcal{S}}. \tag{6}$$

Next, we present set-propagation approaches, which do not require to perform intersections.

2.5. Set-propagation observers

A disadvantage of the strip-based approach is that efficient set representations, such as ellipsoids and zonotopes, are not closed under intersection. Set-propagation approaches eliminate this problem, which are typically based on the update equation of a Luenberger observer:

$$\hat{x}_{k+1} = A\hat{x}_k + Bu_k + w_k + L(y_k - C\hat{x}_k - v_k), \tag{7}$$

where $\hat{x}_{k+1}$ is the estimated state at step $k+1$. The observer gain L is designed so that the estimated state quickly converges to the true state. A simple and direct way to obtain guaranteed state estimation is to evaluate (7) in a set-based fashion (Combastel, 2015b, Sec. 4.1):

$$\mathcal{S}_{k+1} = (A - LC)\mathcal{S}_k \oplus Bu_k \oplus Ly_k \oplus (-L)\mathcal{V} \oplus \mathcal{W}. \tag{8}$$

[2] Please note that, in some other works, the order of a zonotope is defined as r, see, e.g., Alamo et al. (2005, Sec. 4.1), (Bravo, Alamo, & Camacho, 2006, Def. 6).

Table 1
Comparison of set representations for unreduced results when the linear map $M\mathcal{S}$ is performed with a square matrix M of full rank ($\boldsymbol{\times}$: not closed under set operation).

Set representation	Linear map	Mink. sum	Intersection
H-Polytopes (spanned by n generators)	$\mathcal{O}(n^3)$ † (Bogomolov et al., 2018, Tab. 1)	$\mathcal{O}(2^n)$ (Bogomolov et al., 2018, Tab. 1)	$\mathcal{O}(1)$ Eq. (1)
V-Polytopes (spanned by n generators)	$\mathcal{O}(n^2 2^n)$ (Bogomolov et al., 2018, Tab. 1)	$\mathcal{O}(n2^{2n})$ (Bogomolov et al., 2018, Tab. 1)	Super-polynomial [a] (Bremner, 1997, Ch. 6.1)
Ellipsoids	$\mathcal{O}(n^3)$ (Kurzhanskiy & Varaiya, 2006, Sec. 2.2.1)	$\boldsymbol{\times}$	$\boldsymbol{\times}$
Zonotopes (n generators)	$\mathcal{O}(n^3)$ (Althoff & Frehse, 2016, Tab. I)	$\mathcal{O}(n)$ (Althoff & Frehse, 2016, Tab. I)	$\boldsymbol{\times}$

[a] Intersection has to be performed by facet and vertex enumeration.

It is fairly easy to see that (8) is over-approximative if $\hat{x}_0 \in \mathcal{S}_0$ and $\mathcal{V}$ as well as $\mathcal{W}$ contain the origin: The true solution is $x_{k+1} = Ax_k + Bu_k + w_k$ according to (7). Since $\mathcal{V}$ and $\mathcal{W}$ contain the origin, their set-based evaluation only inflates the true evolution of the state so that the state inclusion holds for any L. The matrix gain L can thus be used to optimize the estimation accuracy based on cost functions from Section 2.2, either offline (constant gain) or online (time-varying gain).

2.6. Interval observers

Yet another possibility to avoid intersections is to bound the state by two observers when exploiting monotonicity of the system dynamics (Tang et al., 2019, Sec. VI). Since often the dynamics is not monotone, a new method is presented in Tang et al. (2019, Alg. 1), which is proven to be at least as good as the classical interval observers exploiting monotonicity. The proposed approach in Alg. 1 is based on (8) and avoids the wrapping effect by rearranging the computation of (8) and using the box operator analogously to Girard, Le Guernic, and Maler (2006).

Algorithm 1 Interval observer from Tang et al. (2019, Alg. 1).

Input: input sequence u_k, output sequence y_k
Output: Sequence of state bounds $\underline{x}_k$, $\overline{x}_k$.

$\hat{x}_0 \leftarrow \text{CENTER}(\mathcal{X}_0)$, $\mathcal{D}_0 \leftarrow \mathcal{W} \oplus (-L)\mathcal{V}$
$\mathcal{S}_{x,0} \leftarrow \mathcal{X}_0$, $\mathcal{S}_{wv,0} \leftarrow \mathbf{0}$
for all $k \geq 0$ **do**
  $[\underline{e}_k, \overline{e}_k] = \text{BOX}(\mathcal{S}_{x,k}) \oplus \mathcal{S}_{wv,k}$
  $[\underline{x}_k, \overline{x}_k] = \hat{x}_k + [\underline{e}_k, \overline{e}_k]$
  $\hat{x}_{k+1} = A\hat{x}_k + Bu_k + L(y_k - C\hat{x}_k)$
  $\mathcal{S}_{x,k+1} = (A - LC)\mathcal{S}_{x,k}$
  $\mathcal{S}_{wv,k+1} = \mathcal{S}_{wv,k} \oplus \text{BOX}(\mathcal{D}_k)$
  $\mathcal{D}_{k+1} = (A - LC)\mathcal{D}_k$
end for

2.7. Summary

In Wang et al. (2018b, Sec. 5) it has been shown that there exists a parameterization for the set-propagation approach and the strip-based approach such that both approaches produce exactly the same result. However, no general procedure is known that converts one approach into the other one. Given a state-of-the art parameterization of each method, it is unclear which method performs better in which application. We try to shed some light into this question in this paper. Next, we present concrete realizations of the presented observer types when using zonotopes as a set representation.

Strip-based observers can only finish their computation of the estimated set $\mathcal{S}_k$ after receiving the measurement y_k. As a consequence, the estimated set $\mathcal{S}_k$ arrives with a delay. This problem does not occur when using set-propagation observers and interval observes, which obtain $\mathcal{S}_k$ before time step k when the implementation is real-time capable. To retain formal correctness, it would be required for strip-based observers to additionally compute a one-step prediction of the set of states and use this set as the set of initial states as shown in Schürmann et al. (2018, Sec. III). Since some practitioners may want to ignore the delayed computation (e.g. in a fault-detection algorithm), we list the computation times in Table 3 without the additional prediction step, but indicate that these algorithms are not necessarily ready to be used for control. Our experiments have shown that adding a second prediction would roughly increase the computation in Table 3 by 0.1 ms.

3. Zonotopic observers

As shown in Section 2, guaranteed state estimation mainly requires linear maps, Minkowski sums, and intersections. While constrained zonotopes are closed under these operations, they require solving linear programs to obtain ranges of state intervals. A comparison between the remaining set representations, namely ellipsoids, zonotopes, and polytopes, is shown in Table 1 for the mentioned operations. We assume that the resulting sets in Table 1 are not reduced, e.g., redundant inner points of a V-polytope are not removed.

It can be seen from Table 1 that zonotopes provide higher accuracy compared to using ellipsoids and lower computational complexity compared to polytopes. Thus, we will only present zonotopic observers in this section; we assume that the set of initial states $\mathcal{X}_0$, the set of disturbances $\mathcal{W}$, and the set of noises $\mathcal{V}$ are bounded by zonotopes. If these sets are not zonotopes, one could over-approximate them by zonotopes.

3.1. Strip-based observers

Strip-based observers using zonotopes only differ in the way the intersection in (5) and (6) is over-approximated after obtaining the predicted zonotope $\mathcal{S}^p = c^p \oplus G^p\mathcal{B}^r$. A graphical representation of the intersection methods is presented in Fig. 1, which are briefly introduced subsequently.

Intersection method I: By considering the multi-output system (2) as n_y separate single-output systems, the intersection of the predicted zonotope $\mathcal{S}^p$ and the first strip $\hat{\mathcal{S}}_1$ in (4) can be over-approximated by a family of zonotopes parameterized by $\lambda^1 \in \mathbb{R}^n$ (Alamo et al., 2005, Sec. 6) (Le et al., 2013b, Sec. 4):

$$\hat{\mathcal{Z}}_1(\lambda^1) = (I - \lambda^1 C_1)c^p + \lambda^1 y_{k,1} \oplus [(I - \lambda^1 C_1)G^p,\ \lambda^1\sigma_1]\mathcal{B}^{r+1},$$

where I is the identity matrix of proper dimension. The resulting zonotope is then intersected with the strip $\hat{\mathcal{S}}_2$ corresponding to the second output. This procedure is repeated until the last

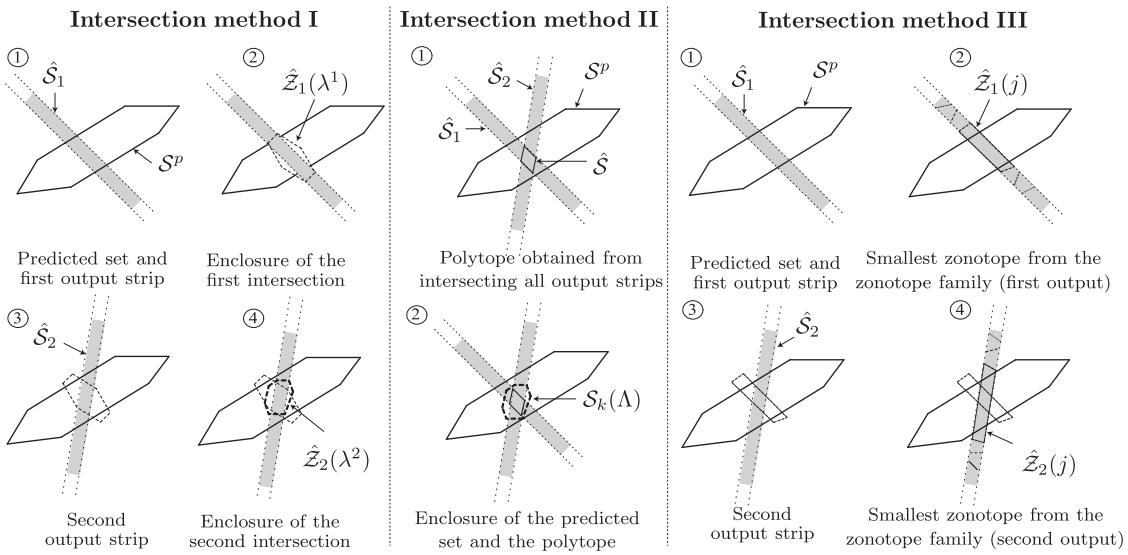

Fig. 1. Graphical representation of all intersection methods for the multi-output case.

Table 2
Combinations of intersection methods and cost functions.

Inter- section	Cost function		
	Volume	F-radius	P-radius
I	VolMin-A (Alamo et al., 2005)	FRad-A (Alamo et al., 2005)	PRad-A (Le et al., 2013b)
II		FRad-B (Wang et al., 2018b)	PRad-B (Le et al., 2013a), PRad-C-I (Wang et al., 2018b), PRad-C-II (Wang, Alamo, Puig and Cembrano, 2018), PRad-D (Wang, Wang, Puig, & Cembrano, 2019)
III	VolMin-B (Bravo et al., 2006)		

measurement to obtain the final estimated set from $\hat{\mathcal{Z}}_{n_y-1} = \hat{c} \oplus \hat{G}\mathcal{B}^{r+n_y-1}$ (Le et al., 2013b, Sec. 4):

$$\mathcal{S}_k = \hat{\mathcal{Z}}_{n_y}(\lambda^{n_y}) = (I - \lambda^{n_y} C_{n_y})\hat{c} + \lambda^{n_y} y_{k,n_y} \oplus [(I - \lambda^{n_y} C_{n_y})\hat{G},\ \lambda^{n_y}\sigma_{n_y}]\mathcal{B}^{r+n_y}.$$

For a compact notation, we store all λ^i in $\Lambda = [\lambda^1, \ldots, \lambda^{n_y}] \in \mathbb{R}^{n \times n_y}$.

Intersection method II: This method (see Le et al. (2013a, Sec. IV)) first computes the exact polytope of the intersections in (5):

$$\hat{\mathcal{S}} = \left\{ x \in \mathbb{R}^n \middle| |Cx - y_k| \leq \sigma \right\}.$$

The intersection with the propagated zonotope in (6) is over-approximated by a zonotope parameterized by Λ (Le et al., 2013a, Sec. IV):

$$\mathcal{S}_k(\Lambda) = (I - \Lambda C)c^p + \Lambda y_k \oplus [(I - \Lambda C)G^p,\ \Lambda\ \mathrm{diag}(\sigma)]\mathcal{B}^{r+n_y},$$

where diag() returns a diagonal matrix.

Intersection method III: The family of zonotopes over-approximating the intersection of $\mathcal{S}^p$ with the first strip according to Bravo et al. (2006, Sec. III.B) is $\hat{\mathcal{Z}}_1(j) = c(j) \oplus G(j)\mathcal{B}^r$ for any integer j, $0 \leq j \leq r$ using the jth column g^j of G^p, where

$$c(j) = \begin{cases} c^p + \frac{y_{k,1} - C_1 c^p}{C_1 g^j} g^j; & \text{if } 1 \leq j \leq r, C_1 g^j \neq 0, \\ c^p; & \text{otherwise,} \end{cases}$$

$$G(j) = \begin{cases} [\tilde{G}_1\ \tilde{G}_2 \ldots \tilde{G}_r]; & \text{if } 1 \leq j \leq r, C_1 g^j \neq 0, \\ G^p; & \text{otherwise,} \end{cases}$$

$$\tilde{G}_o = \begin{cases} g^o - \frac{C_1 g^o}{C_1 g^j}; & \text{if } o \neq j, \\ \frac{\sigma_1}{C_1 g^j} g^j; & \text{if } o = j. \end{cases}$$

Similar to parameterization method I, this zonotope is then intersected with the next strips n_y times until the final estimated zonotopic set $\mathcal{S}_k$ is computed.

To design Λ for intersection methods I and II, and to obtain the optimal bounding zonotope for method III, different cost functions and convex optimization techniques are employed as shown in Table 2. For P-radius minimization, the design parameters in Λ can be obtained by solving the respective optimization problems as bilinear matrix inequalities. For ease of design, the bilinear matrix inequalities can also be solved as a group of linear matrix inequalities by performing a line search or using bisection algorithms (Le et al., 2013a, 2013b). Such an approach reduces the number of decision variables and thus reduces the complexity of solving the linear matrix inequalities.

Irrespective of the parameterization method, all volume minimization and F-radius techniques involve solving an optimization problem in each step during real-time operation. In contrast, Λ is pre-computed before real-time operation for all P-radius techniques.

3.2. Set-propagation observers

We now discuss various techniques for optimizing the observer gain L of (8) for set-propagation observers.

F-radius minimization (FRad-C). Using an analogous procedure as for the Kalman filter, the optimal gain L to minimize the F-radius of $\mathcal{S}_k = c \oplus G\mathcal{B}^r$ is (Combastel, 2015b, Sec. 4.3):

$$L = AGG^T C^T [CGG^T C^T + FF^T]^{-1}.$$

Table 3
Relative rms values υ_i according to (9). Indices of unmeasured states: 1, 3, 6. Indices of measured states: 2, 4, 5 ($\dot{\psi} = a_y/v$).

Technique	Set representation	Ready for control	υ_1	υ_2	υ_3	υ_4	υ_5	υ_6	t_{comp} in [ms]
Strip-based observers									
VolMin-B	Zonotope	✗	4.129	1.000	1.636	1.055	7.136	1.286	131.2
FRad-A	Zonotope	✗	1.854	1.357	2.893	2.619	2.862	1.584	0.546
FRad-B	Zonotope	✗	2.297	1.189	2.878	2.147	2.868	3.124	0.375
PRad-A	Zonotope	✗	8.321	214.8	6.240	21.39	6.154	6.537	0.444
PRad-B	Zonotope	✗	2.583	1.354	1.750	1.464	1.865	4.317	0.252
PRad-C-I	Zonotope	✗	3.239	1.560	6.417	3.438	5.019	3.687	0.259
PRad-C-II	Zonotope	✗	2.460	1.237	1.639	1.064	1.234	4.938	0.268
PRad-D	Zonotope	✗	2.433	1.002	1.641	1.069	1.247	6.539	0.279
CZN-A	constr. zono.	✗	1.010	1.000	1.000	1.000	1.016	1.009	3.412
CZN-B	constr. zono.	✗	1.000	1.000	1.043	1.003	1.000	1.000	3.245
ESO-A	Ellipsoid	✗	3.211	292.8	29.39	94.33	6.554	3.502	1.090
ESO-B	Ellipsoid	✗	4.232	486.0	35.83	177.5	9.418	5.430	1.911
Set-propagation observers									
FRad-C	Zonotope	✓	2.022	32.35	3.315	3.605	3.378	1.926	0.471
PRad-E	Zonotope	✓	2.640	32.03	2.552	2.670	3.166	4.379	0.304
Nom-G	Zonotope	✓	2.702	32.79	2.374	2.293	3.199	4.839	0.258
ESO-C	Ellipsoid	✓	1.995	65.90	7.554	4.811	5.184	4.463	0.052
ESO-D	Ellipsoid	✓	10.83	372.5	42.82	27.25	29.28	25.92	0.051
Interval observer									
Hinf-G	Zonotope	✓	2.669	37.26	3.456	3.298	3.929	3.522	0.251
Smallest absolute radii									
			0.139	0.006	0.061	0.094	0.082	3.236	

P-radius minimization (PRad-E). The observer gain L minimizing the P-radius of $\mathcal{S}_k$ is (Wang et al., 2017, eq. 17):

$$L = P^{*-1}Q, \quad P^* = \text{argmax}(\text{trace}(P))$$

subject to

$$\begin{bmatrix} -\beta P & 0 & 0 & A^TP - C^TQ^T \\ \star & -E^TE & 0 & E^TP \\ \star & \star & -F^TF & F^TQ^T \\ \star & \star & \star & -P \end{bmatrix} \prec 0,$$

where $\star$ is a term that can be induced by symmetry, $\beta \in]0, 1[$ is a design parameter, $Q \in \mathbb{R}^{n \times n_y}$, and $P = P^T \succ 0$ is a symmetric positive definite matrix.

Nominal gain design (Nom-G). For the nominal form of the linear system (2), i.e., in the absence of disturbances and noises, the observer gain L can be designed as (Wang et al., 2018b, eq. (36))

$$L = P^{-1}Y,$$

where $P = P^T \succ 0$ is a symmetric positive definite matrix and $Y \in \mathbb{R}^{n \times n_y}$ has to fulfill

$$\begin{bmatrix} \mu P & \star \\ PA - YC & P \end{bmatrix} \succ 0$$

for a scalar $\mu \in]0, 1]$. The observer gain is stable with a decay rate μ for the nominal form of the system.

3.3. Interval observer

We only consider one approach to design the observer gain L in Alg. 1.

H-infinity-based design (Hinf-G). A H-infinity-based optimization problem to find L is devised in Tang et al. (2019, eq. 16):

$$\min_{\gamma} \ \gamma^2$$

subject to

$$\begin{bmatrix} I - P & \star & \star & \star \\ 0 & -\gamma^2 I & \star & \star \\ 0 & 0 & -\gamma^2 I & \star \\ PA - YC & PE & -YF & -P \end{bmatrix} \prec 0,$$

where $Y = PL$, $\gamma > 0$ is a scalar, and $P = P^T \succ 0$ is a symmetric positive definite matrix. The observer gain is thus computed such that the estimation error is robust against disturbances and noise influences.

3.4. Summary

The design of the observer gain L is computed at each step using the FRad-C technique, while for PRad-E, Nom-G, and Hinf-G, the gain L is pre-computed off-line. Considering all the zonotopic state observers discussed earlier, the order of the zonotopic estimation set $\mathcal{S}_k$ increases with k irrespective of the design approach. To circumvent this problem, several zonotope order-reduction techniques (Althoff, 2010; Combastel, 2003; Girard, 2005; Kopetzki, Schürmann, & Althoff, 2017; Kühn, 1998; Yang & Scott, 2018) have been proposed to bound the higher-order zonotope by a lower-order one, where Kühn (1998) proposed the first approach and Combastel (2003) first reduced zonotopes by sorting generators. These methods are analyzed in our subsequent performance evaluation.

4. Performance evaluation

In this section, we evaluate the performance of the presented zonotopic observers and compare them with the following observers using ellipsoids and constrained zonotopes:

(1) A strip-based observer with optimal bounding ellipsoids (ESO-A), where the intersection with the measurement set is performed according to Gollamudi et al. (1996) and the prediction step according to Liu, Zhao, and Wu (2016). When using the prediction approach in Gollamudi et al. (1996), the results would have been too over-approximative.
(2) A strip-based observer with selective observation update for linear-disturbed systems (ESO-B) (Liu et al., 2016).
(3) An ellipsoidal set-propagation observer using ellipsoidal invariant sets for error estimation (ESO-C) (Loukkas, Martinez, & Meslem, 2017).
(4) A robust H-infinity-based ellipsoidal interval observer (ESO-D) (Martinez, Loukkas, & Meslem, 2020).

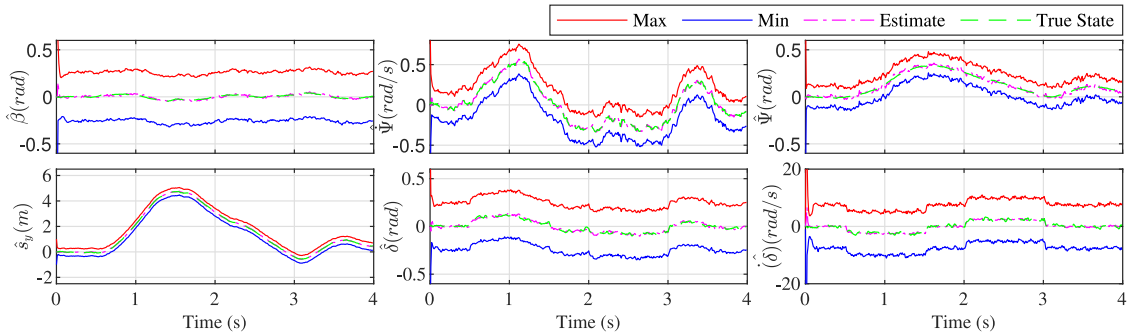

Fig. 2. Estimated interval centers and bounds for all states using the FRad-A technique.

(5) A constrained zonotopic observer with direct intersection (CZN-A) (Scott et al., 2016).
(6) A constrained zonotopic observer with strip-based intersection optimized using F-radius minimization (CZN-B) (Alanwar et al., 0000).

All ellipsoids (initial set, disturbance set, and sensor noise set) are chosen so that they are enclosed in the corresponding zonotopes. We evaluated all observers on an Intel(R) Core(TM) i7-8565U CPU @ 1.80 GHz machine with MATLAB 2020b with single thread executions.[3] For all set operations we have used the CORA toolbox (Althoff, 2015) and optimization problems have been solved using the YALMIP toolbox (Lofberg, 0000) with the Mosek solver (MOSEK, 2015).

4.1. Performance metrics

We evaluate all observers with respect to tightness of the estimated sets and computation time. The relative rms (root-mean-square) values of the interval radius $r_{i,k,l}$ of the ith state variable at step k out of N_s time steps of observer l are computed as:

$$\upsilon_{i,l} = \frac{\tilde{r}_{i,l}}{\min(\tilde{r}_{i,1}, \ldots, \tilde{r}_{i,n_l})}, \quad \tilde{r}_{i,l} = \sqrt{\left(\frac{1}{N_s}\sum_{k=0}^{N_s-1} r_{i,k,l}^2\right)}. \tag{9}$$

We are not using volume as a metric due to its computational complexity for zonotopes (see Alamo et al. (2005, Sec. 6.2)); also, volume approximation methods for zonotopes are not yet accurate enough.

4.2. Case study

We consider the case study of estimating states of an autonomous vehicle. Typically, the yaw rate and the longitudinal velocity of the vehicle are measurable (Wang et al., 2015). Using these measurements, the lateral acceleration of the vehicle can also be computed. However, the lateral velocity or side slip are difficult to measure (Soualmi, Sentouh, Popieul, & Debernard, 2014; Wang et al., 2015), which are important values for safe motion planning of autonomous vehicles. Due to the safety-criticality of autonomous vehicles, it is essential that we reconstruct the set of possible states instead of a single estimate.

We use the vehicle model in Althoff, Koschi, and Manzinger (2017) and combine it with the steer column dynamics in Soualmi et al. (2014) to obtain an Euler-discretized model in the form of (2) for a sampling time of $T_s = 10$ milliseconds (ms). The system states are $x_{v6} = [\tilde{\beta}, \dot{\Psi}, \Psi, s_y, \delta, \dot{\delta}]^T$, where $\tilde{\beta}, \Psi$ are the side slip and yaw angles in radian, s_y is the lateral displacement in m, $\dot{\Psi}$ is the yaw rate in radian/s, δ is the steer angle in radian and $\dot{\delta}$ is the steer rate in radian/s. The initial state is chosen as the origin, the control output u_k is the steering torque from the motor of the electronic power steering unit, and the measurements y_k are the lateral acceleration a_y, steering angle δ, and vehicle lateral position s_y from the lane center line (Rajamani, Tan, Law, & Zhang, 2000). For space reasons, the system equations and the set of disturbances and sensor noises can only be found online.[3]

We consider a double-lane change maneuver executed at a fixed longitudinal velocity of 15 m/s. To analyze the scalability of various set-based observers, we also consider reduced-order vehicle systems with the respective state vectors $x_{v4} = [\tilde{\beta}, \dot{\Psi}, \Psi, s_y]^T$ and $x_{v2} = [\tilde{\beta}, \dot{\Psi}]^T$. For all these vehicular systems, the side slip angle is not measurable and thus estimated. It was observed that the performance of most observers showed no significant variations with respect to the dimension of the vehicular system so that we only present the results of the full system. The results of the other models are provided online.[3]

4.3. Results

The performance metrics from Section 4.1 are listed in Table 3, where t_{comp} is the computation time per iteration in milliseconds (ms). Since VolMin-A has extremely high computational costs, we could only apply it to the smallest vehicle model and thus it is missing in Table 3. As examples, we visualize the estimated intervals of all states using the FRad-A observer in Fig. 2, the FRad-C observer in Fig. 3, and the Hinf-G observer in Fig. 4.

We have also analyzed the effect of using different order reduction techniques. Overall, order reduction has only a limited effect (i.e., less than 18% change in interval radii of measured states). Due to the limited influence on the best observers we only present these results online.[3]

Zonotopes or constrained zonotopes or ellipsoids?

- *Tightness*: Since constrained zonotopes are closed under linear maps, Minkowski sum, and intersection, they provide the tightest results as shown in Table 3. However, one cannot directly compute their intervals for a given variable since this requires solving linear programs (Scott et al., 2016, eq. (25),(26)), which cannot be solved in real time for the considered problem. In contrast, intervals of zonotopes and ellipsoids can be easily obtained. The estimated interval radii of zonotopic observers are significantly tighter than those of ellipsoidal observers, irrespective of the used method; see Table 3. The worst zonotopic strip-based observer PRad-A has a better accuracy than the best ellipsoidal strip-based observer ESO-A. Likewise, the worst zonotopic set-propagation observer Nom-G is more accurate than the best ellipsoidal set-propagation observer ESO-C.

[3] The implementation files for all set-based observers discussed in this paper and further results are provided at https://MatthiasAlthoff@bitbucket.org/MatthiasAlthoff/set-based-observer-comparison-lti-2021.git.

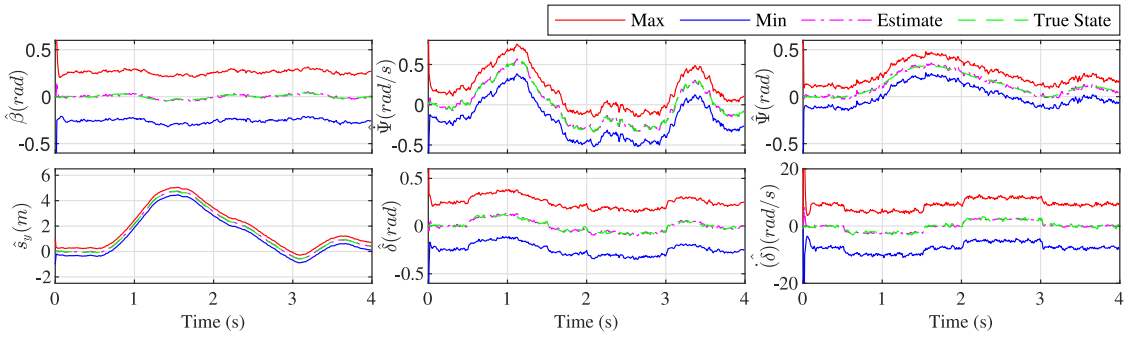

Fig. 3. Estimated interval centers and bounds for all states using the FRad-C technique.

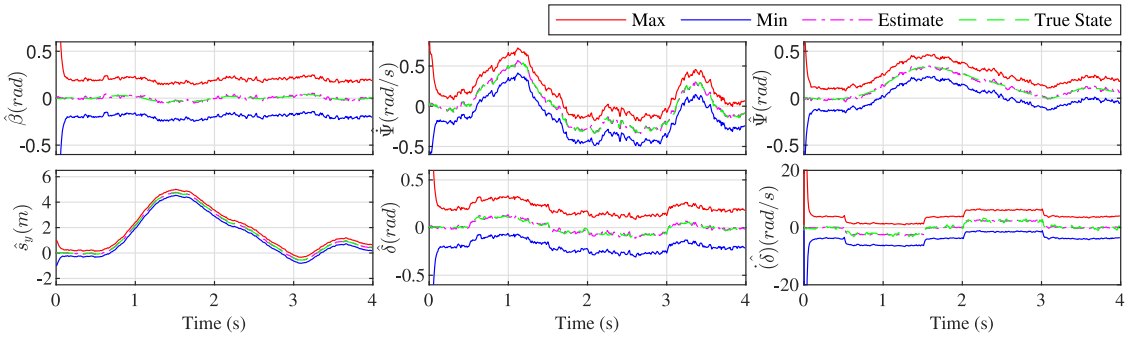

Fig. 4. Estimated interval centers and bounds for all states using the Hinf-G technique.

- *Computational efficiency*: The computational costs of ellipsoidal observers are roughly an order of magnitude lower for set-propagation techniques compared to zonotopic observers in Table 3. However, for strip-based techniques, the computation times are more similar. Constrained zonotopes have a larger computation time compared to the other set representations, except for VolMin-B. This time is significantly enlarged by 492 ms per time step when the interval of values for a specific variable is required (zonotopes: 0.1 ms. ellipsoids: 6.6 ms).

Strip-based or set-propagation or interval observer?

- *Tightness*: Except PRad-A, all zonotopic strip-based observers have an average relative radius below 4 in Table 3, while no zonotopic set-propagation observer has an average relative score below 4.
- *Computational efficiency*: The fastest computational times have been obtained for set-propagation observers when using ellipsoids. However, also when using zonotopes, set-propagation observers are slightly faster compared to the other observer types as shown in Table 3. All approaches have similar computational costs and are real-time capable ($t_{cp} < 10$ ms; step size is 10 ms), except VolMin-B. Obviously, the computational time of observers requiring real-time updates of design parameters, i.e., FRad-A, FRad-B, FRad-C, ESO-A, and ESO-B are slightly higher than the P-radius techniques, where the design gains are precomputed.
- *Ratio of tightness compared to computational efficiency*: A particularly good ratio of tightness compared to computational efficiency has been obtained by PRad-B and PRad-C-II in our use case.

5. Conclusions

Irrespective of the design approach, zonotopic observers outperform ellipsoidal observers in terms of tightness. While constrained zonotopic observers are even tighter, computing the intervals of state variables requires solving linear programs, rendering them only practical when explicit bounds for state variables are not required. Regarding computational costs, ellipsoidal observers have significantly lower computational costs than zonotopic observers when using set-propagation designs. All presented observers, except those based on volume minimization, can be implemented in real-time for the considered automotive systems. We also observed that zonotope reduction techniques had only a minor impact on the overall performance. A particularly good ratio of tightness compared to computational efficiency has been obtained by PRad-B and PRad-C-II in our use case. Due to the recent progress, more real-world applications would be commendable. When the application does not accept delays in the result of guaranteed bounds, set propagation techniques should be used. If the application requires explicit bounds for individual state variables, zonotopes should be selected. Finally, we would like to stress that we only focused on linear time-invariant systems. For linear time-varying systems and nonlinear systems, the performance of certain concepts might shift substantially.

References

Alamo, T., Bravo, J. M., & Camacho, E. F. (2005). Guaranteed state estimation by zonotopes. *Automatica*, *41*(6), 1035–1043.

Alanwar, A., Gassmann, V., He, X., Said, H., Sandberg, H., Johansson, K. H., & Althoff, M. Privacy preserving set-based estimation using partially homomorphic encryption. arXiv:2010.11097.

Althoff, M. (2010). *Reachability analysis and its application to the safety assessment of autonomous cars* (Dissertation), Technische Universität München, http://nbn-resolving.de/urn/resolver.pl?urn:nbn:de:bvb:91-diss-20100715-963752-1-4.

Althoff, M. (2015). An introduction to CORA 2015. In *Proc. of the workshop on applied verification for continuous and hybrid systems* (pp. 120–151).

Althoff, M., & Dolan, J. M. (2014). Online verification of automated road vehicles using reachability analysis. *IEEE Transactions on Robotics*, *30*(4), 903–918.

Althoff, M., & Frehse, G. (2016). Combining zonotopes and support functions for efficient reachability analysis of linear systems. In *Proc. of the 55th IEEE conference on decision and control* (pp. 7439–7446).

Althoff, M., Koschi, M., & Manzinger, S. (2017). CommonRoad: Composable benchmarks for motion planning on roads. In *Proc. of the IEEE intelligent vehicles symposium* (pp. 719–726).

Althoff, M., Stursberg, O., & Buss, M. (2008). Reachability analysis of nonlinear systems with uncertain parameters using conservative linearization. In *Proc. of the 47th IEEE conference on decision and control* (pp. 4042–4048).

Bertsekas, D. P., & Rhodes, I. B. (1971). Recursive state estimation for a set-membership description of uncertainty. *IEEE Transactions on Automatic Control*, *16*, 117–128.

Blanchini, F., & Miani, S. (2008). *Set-theoretic methods in control* (pp. 73–97). Boston: Birkhäuser.

Blesa, J., Puig, V., Romera, J., & Saludes, J. (2011). Fault diagnosis of wind turbines using a set-membership approach. *IFAC Proceedings Volumes*, *44*(1), 8316–8321.

Blesa, J., Rotondo, D., Puig, V., & Nejjari, F. (2014). FDI and FTC of wind turbines using the interval observer approach and virtual actuators/sensors. *Control Engineering Practice*, *24*, 138–155.

Bogomolov, S., Forets, M., Frehse, G., Viry, F., Podelski, A., & Schilling, C. (2018). Reach set approximation through decomposition with low-dimensional sets and high-dimensional matrices. In *Proc. of the 21st international conference on hybrid systems: Computation and control* (pp. 41–50).

Bravo, J. M., Alamo, T., & Camacho, E. F. (2006). Bounded error identification of systems with time-varying parameters. *IEEE Transactions on Automatic Control*, *51*(7), 1144–1150.

Bremner, D. D. (1997). *On the complexity of vertex and facet enumeration for convex polytopes (Dissertation)*. McGill University.

Chabane, S. Ben (2015). *Fault detection techniques based on set-membership state estimation for uncertain systems* (Dissertation), Université Paris-Saclay.

Chisci, L., Garulli, A., & Zappa, G. (1996). Recursive state bounding by parallelotopes. *Automatica*, *32*(7), 1049–1055.

Combastel, C. (2003). A state bounding observer based on zonotopes. In *Proc. of the European control conference*(pp. 2589–2594).

Combastel, C. (2005). A state bounding observer for uncertain non-linear continuous-time systems based on zonotopes. In *Proc. of the 44th IEEE conference on decision and control, and the European control conference* (pp. 7228–7234).

Combastel, C. (2015a). Merging Kalman filtering and zonotopic state bounding for robust fault detection under noisy environment. *IFAC-PapersOnLine*, *48*(21), 289–295.

Combastel, C. (2015b). Zonotopes and Kalman observers: Gain optimality under distinct uncertainty paradigms and robust convergence. *Automatica*, *55*, 265–273.

Durieu, C., Walter, É., & Polyak, B. (2001). Multi-input multi-output ellipsoidal state bounding. *Journal of Optimization Theory and Applications*, *111*(2), 273–303.

Efimov, D., Raïssi, T., Chebotarev, S., & Zolghadri, A. (2013). Interval state observer for nonlinear time varying systems. *Automatica*, *49*(1), 200–205.

Falcone, P., Ali, M., & Sjöberg, J. (2011). Predictive threat assessment via reachability analysis and set invariance theory. *IEEE Transactions on Intelligent Transportation Systems*, *12*(4), 1352–1361.

Girard, A. (2005). Reachability of uncertain linear systems using zonotopes. In *LNCS*: *vol. 3414*, *Hybrid systems: Computation and control* (pp. 291–305). Springer.

Girard, A., Le Guernic, C., & Maler, O. (2006). Efficient computation of reachable sets of linear time-invariant systems with inputs. In *LNCS*: *vol. 3927*, *Hybrid systems: Computation and control* (pp. 257–271). Springer.

Gollamudi, S., Nagaraj, S., Kapoor, S., & Huang, Y. F. (1996). Set-membership state estimation with optimal bounding ellipsoids. In *Proc. of the international symposium on information theory and its applications* (pp. 262–265).

Gouzé, J. L., Rapaport, A., & Hadj-Sadok, M. Z. (2000). Interval observers for uncertain biological systems. *Ecological Modelling*, *133*(1), 45–56.

Kochdumper, N., Tarraf, A., Rechmal, M., Olbrich, M., Hedrich, L., & Althoff, M. (2020). Establishing reachset conformance for the formal analysis of analog circuits. In *Proc. of the 25th Asia and South Pacific design automation conference* (pp. 199–204).

Kopetzki, A.-K., Schürmann, B., & Althoff, M. (2017). Methods for order reduction of zonotopes. In *Proc. of the 56th IEEE conference on decision and control* (pp. 5626–5633).

Kostousova, E. K. (1998). State estimation for dynamic systems via parallelotopes optimization and parallel computations. *Optimization Methods & Software*, *9*(4), 269–306.

Kühn, W. (1998). Rigorously computed orbits of dynamical systems without the wrapping effect. *Computing*, *61*, 47–67.

Kurzhanskiy, A. A., & Varaiya, P. (2006). *Ellipsoidal toolbox*: *Technical Report UCB/EECS-2006-46*, Berkeley: EECS Department, University of California.

Le, V. T. H., Alamo, T., Camacho, E. F., Stoica, C., & Dumur, D. (2011). A new approach for guaranteed state estimation by zonotopes. *IFAC Proceedings Volumes*, *44*(1), 9242–9247.

Le, V. T. H., Alamo, T., Camacho, E. F., Stoica, C., & Dumur, D. (2012). Zonotopic set-membership estimation for interval dynamic systems. In *Proc. of the IEEE American control conference* (pp. 6787–6792).

Le, V. T. H., Stoica, C., Alamo, T., Camacho, E. F., & Dumur, D. (2013a). Zonotope-based set-membership estimation for Multi-Output uncertain systems. In *Proc. of the IEEE international symposium on intelligent control* (pp. 212–217).

Le, V. T. H., Stoica, C., Alamo, T., Camacho, E. F., & Dumur, D. (2013b). Zonotopic guaranteed state estimation for uncertain systems. *Automatica*, *49*(11), 3418–3424.

Le, V. T. H., Stoica, C., Dumur, D., Alamo, T., & Camacho, E. F. (2011). Robust tube-based constrained predictive control via zonotopic set-membership estimation. In *Proc. of the IEEE conference on decision and control and European control conference* (pp. 4580–4585).

Limon, D., Alvarado, I., Alamo, T., & Camacho, E. F. (2010). Robust tube-based MPC for tracking of constrained linear systems with additive disturbances. *Journal of Process Control*, *20*(3), 248–260.

Liu, S. B., & Althoff, M. (2018). Reachset conformance of forward dynamic models for the formal analysis of robots. In *Proc. of the IEEE/RSJ international conference on intelligent robots and systems* (pp. 370–376).

Liu, Y., Zhao, Y., & Wu, F. (2016). Ellipsoidal state-bounding-based set-membership estimation for linear system with unknown-but-bounded disturbances. *IET Control Theory & Applications*, *10*(4), 431–442.

Lofberg, J. YALMIP : a toolbox for modeling and optimization in MATLAB. In *Proc. of the IEEE international conference on robotics and automation* (pp. 284–289).

Loukkas, N., Martinez, J. J., & Meslem, N. (2017). Set-membership observer design based on ellipsoidal invariant sets. *IFAC-Papers On Line*, *50*(1), 6471–6476.

Martinez, J. J., Loukkas, N., & Meslem, N. (2020). H_∞ set-membership observer design for discrete-time LPV systems. *International Journal of Control*, *93*(10), 2314–2325.

Mazenc, F., & Bernard, O. (2011). Interval observers for linear time-invariant systems with disturbances. *Automatica*, *47*(1), 140–147.

Mitra, S., Wongpiromsarn, T., & Murray, R. M. (2013). Verifying cyber-physical interactions in safety-critical systems. *IEEE Security and Privacy*, *11*(4), 28–37.

MOSEKApS (2015). The MOSEK optimization toolbox for MATLAB manual. Version 7.1 (revision 28).

Polyak, B. T., Nazin, S. A., Durieu, C., & Walter, E. (2004). Ellipsoidal parameter or state estimation under model uncertainty. *Automatica*, *40*(7), 1171–1179.

Pourasghar, M., Puig, V., & Ocampo-Martinez, C. (2016). Comparison of set-membership and interval observer approaches for state estimation of uncertain systems. In *Proc. of the IEEE European control conference* (pp. 1111–1116).

Pourasghar, M., Puig, V., & Ocampo-Martinez, C. (2019). Interval observer versus set-membership approaches for fault detection in uncertain systems using zonotopes. *International Journal of Robust and Nonlinear Control*, *29*(10), 2819–2843.

Puig, V. (2010). Fault diagnosis and fault tolerant control using set-membership approaches: Application to real case studies. *International Journal of Applied Mathematics and Computer Science*, *20*, 619–635.

Puig, V., Cuguero, P., & Quevedo, J. (2001). Worst-case state estimation and simulation of uncertain discrete-time systems using zonotopes. In *Proc. of the IEEE European control conference* (pp. 1691–1697).

Raïssi, T., & Efimov, D. (2018). Some recent results on the design and implementation of interval observers for uncertain systems. *Automatisierungstechnik*, *66*(3), 213–224.

Rajamani, R., Tan, H. S., Law, B. K., & Zhang, W. B. (2000). Demonstration of integrated longitudinal and lateral control for the operation of automated vehicles in platoons. *IEEE Transactions on Control Systems Technology*, *8*(4), 695–708.

Rajkumar, R., Lee, I., Sha, L., & Stankovic, J. (2010). Cyber-physical systems: The next computing revolution. In *Proc. of the 47th design automation conference* (pp. 731–736).

Rego, B. S., Raffo, G. V., Scott, J. K., & Raimondo, D. M. (2020). Guaranteed methods based on constrained zonotopes for set-valued state estimation of nonlinear discrete-time systems. *Automatica*, *111*, Article 108614.

Rego, B. S., Raimondo, D. M., & Raffo, G. V. (2018). Path tracking control with state estimation based on constrained zonotopes for aerial load transportation. In *Proc. of the 57th IEEE conference on decision and control* (pp. 1979–1984).

Roehm, H., Oehlerking, J., Woehrle, M., & Althoff, M. (2016). Reachset conformance testing of hybrid automata. In *Proc. of hybrid systems: Computation and control* (pp. 277–286).

Roehm, H., Oehlerking, J., Woehrle, M., & Althoff, M. (2019). Model conformance for cyber-physical systems: A survey. *ACM Transactions on Cyber-Physical Systems*, *3*(3), Article 30.

Schürmann, B., Kochdumper, N., & Althoff, M. (2018). Reachset model predictive control for disturbed nonlinear systems. In *Proc. of the 57th IEEE conference on decision and control* (pp. 3463–3470).

Schweppe, F. (1968). Recursive state estimation: Unknown but bounded errors and system inputs. *IEEE Transactions on Automatic Control*, *13*(1), 22–28.
Scott, J. K., Raimondo, D. M., Marseglia, G. R., & Braatz, R. D. (2016). Constrained zonotopes: A new tool for set-based estimation and fault detection. *Automatica*, *69*, 126–136.
Soualmi, B., Sentouh, C., Popieul, J. C., & Debernard, S. (2014). Automation-driver cooperative driving in presence of undetected obstacles. *Control Engineering Practice*, *24*, 106–119.
Tang, W., Wang, Z., Shen, Y., Rodrigues, M., & Theilliol, D. (2018). Fault detection based on multi-objetcive observer and interval hull computation. *IFAC Papers Online*, *51*(24), 332–337.
Tang, W., Wang, Z., Wang, Y., Raïssi, T., & Shen, Y. (2019). Interval estimation methods for discrete-time linear time-invariant systems. *IEEE Transactions on Automatic Control*, *64*(11), 4717–4724.
Wang, Y., Alamo, T., Puig, V., & Cembrano, G. (2018). A distributed set-membership approach based on zonotopes for interconnected systems. In *Proc. of the IEEE conference on decision and control* (pp. 668–673).
Wang, Y., Bevly, D. M., & Rajamani, R. (2015). Interval observer design for LPV systems with parametric uncertainty. *Automatica*, *60*, 79–85.
Wang, H., Kolmanovsky, I. V., & Sun, J. (2018). Zonotope-based recursive estimation of the feasible solution set for linear static systems with additive and multiplicative uncertainties. *Automatica*, *95*, 236–245.
Wang, Y., & Puig, V. (2016). Zonotopic extended Kalman filter and fault detection of discrete time nonlinear systems applied to a quadrotor helicopter. In *Proc. of the 3rd IEEE conference on control and fault tolerant systems* (pp. 367–372).
Wang, Y., Puig, V., & Cembrano, G. (2018a). Robust fault estimation based on zonotopic Kalman filter for discrete-time descriptor systems. *International Journal of Robust and Nonlinear Control*, *28*(16), 5071–5086.
Wang, Y., Puig, V., & Cembrano, G. (2018b). Set-membership approach and Kalman observer based on zonotopes for discrete-time descriptor systems. *Automatica*, *93*, 435–443.
Wang, Y., Wang, Z., Puig, V., & Cembrano, G. (2019). Zonotopic set-membership state estimation for discrete-time descriptor LPV systems. *IEEE Transactions on Automatic Control*, *64*(5), 2092–2099.
Wang, Y., Zhou, M., Puig, V., Cembrano, G., & Wang, Z. (2017). Zonotopic fault detection observer with $\mathcal{H}_-$ performance. In *Proc. of the 36th IEEE Chinese control conference* (pp. 7230–7235).
Witheephanich, K., Orihuela, L., Garcia, R. A., & Escano, J. M. (2016). Min-max model predictive control with robust zonotope-based observer. In *Proc. of the UKACC 11th IEEE international conference on control* (pp. 1–6).
Xiong, J. (2013). *Set-membership state estimation and application on fault detection* (Dissertation), Automatique / Robotique. Institut National Polytechnique de Toulouse - INPT.
Yang, X., & Scott, J. K. (2018). A comparison of zonotope order reduction techniques. *Automatica*, *95*, 378–384.
Zheng, G., Efimov, D., & Perruquetti, W. (2016). Design of interval observer for a class of uncertain unobservable nonlinear systems. *Automatica*, *63*, 167–174.

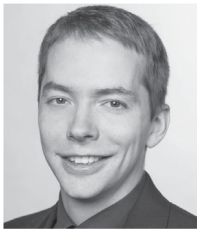

Matthias Althoff is an associate professor in Computer Science at the Technical University of Munich, Germany. He received his diploma engineering degree in Mechanical Engineering in 2005, and his Ph.D. degree in Electrical Engineering in 2010, both from the Technical University of Munich, Germany. From 2010 to 2012 he was a postdoctoral researcher at Carnegie Mellon University, Pittsburgh, USA, and from 2012 to 2013 an assistant professor at Ilmenau University of Technology, Germany. His research interests include the formal verification and analysis of continuous and hybrid systems, reachability analysis, planning algorithms, nonlinear control, automated vehicles, and power systems.

Jagat Jyoti Rath received the B.Tech. degree in electrical engineering from KIIT University, Bhubaneswar, India, in 2010, the M.Tech. degree in mechatronics from Academy of Scientific and Innovative Research, Chennai, India, in 2012, and the Ph.D. degree in embedded systems and control engineering from Kyungpook National University, Daegu, South Korea, in 2016. From 2016-2018, he was a postdoctoral researcher at LAMIH UMR CNRS 8201, Valenciennes, France. From 2019 to 2020, he was a postdoctoral fellow at Technical University of Munich. He has worked on projects related to autonomous driving and human–machine collaborative driving funded by Renault, Ford, Continental among others.

Currently he is an Assistant Professor in the Department of Mechanical and Aero-Space Engineering, Institute of Infrastructure Technology Research and Management (IITRAM), India. His research interests include nonlinear state estimation and control, human–machine interaction management, interval estimation and fault diagnosis/control for mechatronic systems.